Heliyon 10 (2024) e28219

Contents lists available at ScienceDirect

Heliyon

journal homepage: www.cell.com/heliyon

Research article

Effects of a novel *Bacillus subtilis* GXYX crude lipopeptide against *Salmonella enterica* serovar Typhimurium infection in mice

Jingya Zhang [a], Yifan Wu [a], Wei Li [a], Honglin Xie [a], Jingyan Li [b], Yongqiang Miao [a], Zengqi Yang [a], Yefei Zhou [c], Xinglong Wang [a,*]

[a] College of Veterinary Medicine, Northwest A&F University, Yangling, 712100, Shaanxi, China
[b] College of Food Science and Engineering, Northwest A&F University, Yangling, 712100, Shaanxi, China
[c] Department of Life Science, Nanjing Xiaozhuang University, Nanjing, 211171, Jiangsu, China

ARTICLE INFO

Keywords:
Bacillus subtilis
GXYX
Crude lipopeptides
Salmonella enterica serovar typhimurium
Antibacterial activity

ABSTRACT

The increased rate of antibiotic resistance strongly limits the resolution of *Salmonella* enterica serovar Typhimurium (S. Typhimurium) infection. Therefore, new strategies to control bacterial infections are urgently needed. *Bacillus subtilis (B. subtilis)* and its metabolites are desirable antibacterial agents. Here, we aimed to evaluate the antibacterial activity of the novel *B. subtilis* strain GXYX (No: PRJNA940956) crude lipopeptide against *S*. Typhimurium. In vitro, GXYX crude lipopeptides affected *S*. Typhimurium biofilm formation and swimming and attenuated the adhesion and invasion abilities of *S*. Typhimurium toward BHK-21 cells; in addition, it inhibited the mRNA expression of the *filA*, *filC*, *csgA*, and *csgB* genes, which are related to the adhesion and invasion ability of *S*. Typhimurium. In vivo, pretreatment with GXYX crude lipopeptide via intragastric administration improved the survival rate by 30%, which was related to reductions in organ bacterial loads and clinical signs in mice. Intragastric administration of GXYX crude lipopeptide significantly downregulated the mRNA levels of TNF-α, IL-1β, IL-12 and IL-6 in response to *S*. Typhimurium-induced inflammation compared with intraperitoneal injection. Moreover, it significantly improved the intestinal barrier-related gene (ZO-1, claudin-1, occludin-1) mRNA levels in intestinal tissue damaged by S. Typhimurium infection. In conclusion, GXYX crude lipopeptides were effective at reducing *S*. Typhimurium colonization, laying a foundation for the further development of novel antibacterial agents.

1. Introduction

Salmonella enterica serovar Typhimurium (*S*. Typhimurium*)* is a facultative intracellular gram-negative bacterium [1,2]. This pathogen is remarkably adaptive and can invade a variety of host organisms, causing severe economic losses in the animal breeding industry [3]. The problem of *S*. Typhimurium drug resistance is becoming increasingly serious with the extensive use of antibiotics. A

Abbreviations: S. Typhimurium, *Salmonella enterica* serovar Typhimurium; *B. subtilis*, *Bacillus subtilis*; TEM, transmission electron microscopy; MIC, minimum inhibitory concentration; MBC, minimum bactericidal concentration; OG, orogastric gavage; IP, intraperitoneal injection; LD_{50}, 50% lethal dose; RT−qPCR, real-time fluorescence quantitative PCR; H&E, hematoxylin and eosin.

* Corresponding author. College of Veterinary Medicine, Northwest A&F University, No. 22 Xinong Road, Yangling District, Xianyang, 712100, Shaanxi Province, China.
E-mail address: wxlong@nwsuaf.edu.cn (X. Wang).

https://doi.org/10.1016/j.heliyon.2024.e28219
Received 13 August 2023; Received in revised form 12 March 2024; Accepted 13 March 2024
Available online 15 March 2024

total of 39.6% of the 464 strains of *S*. Typhimurium isolated from Morocco were resistant to at least one antibiotic, and the highest tolerance rates were 27.1% for nalididone and 25.0% for sulfonamides [4]. Thus, there is an urgent need to search for novel antibacterial agents. The genus *Bacillus* consists of numerous diverse, gram-positive, rod-shaped bacteria that are generally motile because of their peritrichous flagella [5]. The endospores produced by members of this genus contribute to their survival in unfavorable environments. According to a previous report, the genus *Bacillus* can thrive and produce lipopeptides under high salinity and temperature conditions [6]. Bioactive lipopeptides, which include the surfactin, iturin, and fengycin families, are amphiphilic metabolite-generated *Bacillus* species [7]. Lipopeptides might be effective against bacterial biofilms because of their low toxicity, superior biodegradability and environmental compatibility, high selectivity, foaming capacity and stability in harsh environments [8]. Compared to other peptide antibiotics, lipopeptides seemed to be more effective. They exhibit extremely rigid, hydrophobic and/or cyclic structures that exert potent antibacterial effects and function as multifunctional effector molecules of innate immunity [9]. *Bacillus subtilis* (*B. subtilis*) is one of the most widely used microorganisms for the industrial production of active lipopeptides. Bioactive lipopeptides have been found to inhibit pathogenic organism adhesion by reducing the amount of biofilm formed by *Escherichia coli*, *Proteus mirabilis* and S. Typhimurium [10]. This membrane-lytic process is rapid, physical, irreversible and renders bioactive lipopeptides impregnable to bacteria. Therefore, bioactive lipopeptides are attractive antibacterial agents due to their potential therapeutic effect on drug-resistant organisms.

The novel *B. subtilis* strain GXYX (No: PRJNA940956) was preserved in our laboratory, and its secreted bioactive lipopeptides were called GXYX crude lipopeptides. The aim of this work was to investigate the antibacterial activities of GXYX crude lipopeptides against *S.* Typhimurium in vitro and in vivo.

2. Materials and methods

2.1. Bacteria and cell culture

Salmonella enterica serovar Typhimurium (ATCC14028) was obtained from Shanghai Xin Yu Biotech Co., Ltd. (Shanghai, China) and cultivated in lysogeny broth (LB) culture medium at 220 rpm and 37 °C for further experiments. To construct a bacterial growth curve, the optical density was measured every 1 h at 600 nm (OD600) for 13 h. *Bacillus subtilis* GXYX was isolated from the hog at Northwest A&F University and preserved at −80 °C. BHK-21 cells (baby hamster kidney cell line, ATCC No. CCL-10), a fibroblast-type adherent cell line isolated and cultured from the kidney tissue of Syrian infant hamster (purchased from the American Type Culture Collection [ATCC], CA, VA, USA), were cultured in Dulbecco's modified Eagle's medium (DMEM; Gibco, CA, USA) supplemented with 10% (v/v) fetal bovine serum (FBS; Sijiqing, Hangzhou, China), 20 μg/mL penicillin (Solarbio, Beijing, China) and 20 μg/mL streptomycin (Solarbio, Beijing, China) at 37 °C with 5% CO_2.

2.2. Isolation and identification of the crude lipopeptides of GXYX

Then, 50 μL of *Bacillus subtilis* GXYX glycerin preservation solution was added to 450 μL of lysogeny broth (LB) culture medium to obtain 0.05 (OD600 = 0.05) initial medium, and the OD600 was measured via a spectrophotometer (Cary 60 UV–Vis, Agilent, CA, USA). Two hundred milliliters of initial medium was separated from the 500 mL culture bottle for further culture on a shaking table (TS-200DC, Tiancheng, Shanghai, China) at 220 rpm and 37 °C for 48 h until the OD600 reached 1.75. Then, the culture was centrifuged at 8000×*g* for 30 min to obtain the supernatant. The supernatant was then filtered through Whatman No. 2 filter paper to obtain the filtrate. The filtrate was acidified with 6 N HCl to pH 2.0, placed at 4 °C for 8 h, further centrifuged at 8000×*g* for 30 min to obtain sediment, resuspended in sterile PBS (pH 7.2) three times, centrifuged at 8000×*g* for 30 min to collect sediment, concentrated under vacuum (SCIENTZ-10 N/A, XinZhi, Ningbo, China), and finally dissolved in 5 mL of methanol. Subsequently, the *B. subtilis* fermentation products were subjected to GXYX crude lipopeptide solution [11]. The iturin, surfactin, and fengycin standards used in the study were purchased from Sigma–Aldrich Co. (Sigma–Aldrich, St. Louis, MI, USA). The mobile phases used were Milli-Q water (solvent A) and 0.1% trifluoroacetic acid in acetonitrile (solvent B; Aladdin Reagent, Shanghai, China). All the solvents used were HPLC grade. The crude lipopeptides were prepared and transferred to HPLC vials for injection on the column (Merck, Darmstadt, Germany). The elution of the lipopeptide homologs was monitored at 210 nm. An analytical scale Purospher® RP-C18 (250 × 4.6 mm, 5 μm particle size; Merck, Darmstadt, Germany) column was utilized. All the GXYX crude lipopeptides used in this study were isolated from four batches by shake flask fermentation. One batch of isolated GXYX inoculum (OD600 = 0.05) was added to a 500 mL shake flask containing 200 mL of LB medium and incubated for 48 h at 220 rpm and 37 °C. The yield of one isolate was 2.05 g/L, and the product was dissolved in PBS for further in vivo and in vitro experiments. The dry weight of the lipopeptide was calculated = (weight of tube containing dried lipopeptide − empty tube weight).

2.3. Minimum inhibitory concentration (MIC) and minimum bactericidal concentration (MBC) assays

The MIC of GXYX crude lipopeptides against *S.* Typhimurium was determined by the broth microdilution method. Ten microliters of 1.0 × 10^6 CFU/mL *S*. Typhimurium was incubated with 1 mL of 0.08, 0.16, 0.31, 0.62, 1.25, 2.5, 5, or 10 mg/mL GXYX crude lipopeptide for 24 h at 37 °C, after which the OD600 was measured. The tubes without observable bacterial growth were plated for microbial counting. The minimum concentration of GXYX crude lipopeptide that can inhibit bacterial growth after static incubation for 24 h in a 37 °C incubator (DPX-9052B, Nan Rong, China) was taken as the MIC. To calculate the MBC, a 10 μL aliquot of broth was removed from each tube at concentrations higher than or equivalent to the MIC and statically incubated in LB culture medium at 37 °C

Table 1
The primers used in this study.

Gene	Forward primer (5′–3′)	Reverse primer (5′–3′)
TNF-α	GATGAATGAACGAACAAG	ATCTTCCTCCTTATCTCT
IL-6	ACCTGTCTATACCACTTC	GCATCATCGTTGTTCATA
IL-1β	CAATGGACAGAATATCAAC	ACAGGACAGGTATAGATT
IL-12	AAGATGAAGGAGACAGAG	ATTGGACTTCGGTAGATG
ZO-1	AGCTGCCTCGAACCTCTACTCTAC	GCCTGGTGGTGGAACTTGCTC
Occludin	TGGCTATGGAGGCGGCTATGG	AAGGAAGCGATGAAGCAGAAGGC
Claudin-1	GGTGCCTGGAAGATGATGAGGTG	GCCACTAATGTCGCCAGACCTG
filA	CCGCTGAAGGTGTAATGGAT	CCGCATTTAATAACCCGATG
filC	AACGACGGTATCTCCATTGC	TACACGGTCGATTCCTTCA
csgA	ATGCCCGTAAATCTGAAACG	ACCAACCTGACGCACCATTA
csgB	CGCATGTCGCTAACAAGGTA	ATTATCCGTGCCGACTTGAC
gyrB	CGGTAGTAACGCTCTGTC	GGCCAGAAACGTACCATCGT
β-actin	TTGGGAGGGTGAGGGACT	GAACGGTGAAGGCGACAG

for 24 h. The MBC was determined as the lowest concentration at which no bacterial growth occurred in the subcultures. The data were recorded as the average of triplicate samples.

2.4. Bactericidal kinetic activity

GXYX crude lipopeptides were diluted to 0, 0.3125 (1/2 × MIC), 0.625 (1 × MIC), 1.25 (2 × MIC), and 2.5 mg/mL (4 × MIC), and 50 μL of the diluted solution and an equal volume of *S*. Typhimurium (10^6 CFU/mL) were added to each well of a 96-well plate (Nunc, Roskilde, Denmark). The control samples did not contain GXYX crude lipopeptides. CFUs were counted after incubating for 48 h at 37 °C. The above experiments were conducted in triplicate.

2.5. Bacterial motility test S

Typhimurium was mixed with 0.16, 0.08, or 0.04 mg/mL (1/4, 1/8, or 1/16 × MIC) GXYX crude lipopeptide to a final concentration of 1.0×10^6 CFU and subsequently inoculated in semisolid media (agar concentration (C) = 0.4%). The components of this semisolid medium were 10 g of tryptose, 15 g of NaCl, and 4 g of agar, and the final volume was adjusted to 1000 mL by double distilled water. The pH was adjusted to 7.2 by 0.1 N HCl and NaOH. The diameters of the swimming halos were measured after 24 h of incubation at 37 °C to assess the effects of GXYX crude lipopeptides on the motility of *S*. Typhimurium.

2.6. Biofilm inhibition assay S

Typhimurium (1.0×10^6 CFU/mL) was incubated with or without GXYX crude lipopeptides at 37 °C for 48 h in a sterile 96-well polypropylene plate (Nunc, Roskilde, Denmark). The unbound cells were then washed away with sterilized PBS. Subsequently, the adhered bacteria were fixed using methanol and stained with 0.5% (m/v) crystal violet for 1 min. Thirty-three percent acetic acid was used as the decoloring solution. The absorbance at 590 nm was measured to evaluate biofilm growth [12].

2.7. Transcript levels of adhesion- and invasion-related genes determined by real-time fluorescence quantitative PCR (RT–qPCR) S

Typhimurium (1.0×10^6 CFU/mL) and 0.2 mg/mL GXYX crude lipopeptide were coincubated for 24 h at 37 °C in a static incubator. Total RNA was extracted using TRIzol reagent (Vazyme, Nanjing, China) and reverse transcribed into cDNA via the PrimeScript™ II 1st Strand cDNA Synthesis Kit (TaKaRa, Beijing, China). RT–qPCR was performed on a TL988 Real-Time system (Tianlong, Xian, Shaanxi, China) in triplicate using SYBR Green Master mix (Applied Biosystems, Thermo Fisher Scientific, Inc., Foster City, CA, USA). The mRNA levels of the target genes (filA, filC, csgA, csgB) were normalized to the expression of *gyrB* and calculated using the $2^{-\Delta\Delta CT}$ method by the formula $\Delta\Delta Ct$ = mean ($\Delta Ct_{treated\ sample}$) -mean ($\Delta Ct_{untreated\ sample}$), $\Delta Ct = Ct_{target\ gene} - Ct_{gyrB}$. Mean CT values ± standard deviations are used in the ΔΔCT calculations. The sequences of primers used are listed in Table 1.

2.8. Transmission electron microscopy (TEM) S

Typhimurium (1×10^6 CFU/mL) and GXYX crude lipopeptides (2 × MIC) were incubated at 4 °C for 1 h and fixed in glutaraldehyde (2.5% w/v) at 37 °C for 2 h. Wuhan Service Bio-Technology Co., Ltd. (Wuhan, China) performed the TEM analysis.

2.9. Cytotoxicity assays

The cytotoxicity of GXYX crude lipopeptides was evaluated with a cell counting kit-8 (Beyotime, Haimen, China). Briefly, BHK-21 cell monolayers were incubated with 0.2, 0.4, 0.8, or 2 mg/mL GXYX crude lipopeptide at 37 °C with 5% CO_2 for 24 h. Then, 100 μL/well MTT reagent was added for 2 h of incubation. Subsequently, the formed formazan crystals were dissolved in DMSO (Sigma–

Aldrich, St. Louis, MI, USA). A Biotek ELx800 absorbance microplate reader (BioTek Instruments, WA, USA) was used to measure the absorbance at 570 nm. As viability controls, monolayers without extract were used.

2.10. Anti-invasion and antiadhesion assays

The bacterial killing activity of GXYX crude lipopeptides was assessed by employing a gentamicin protection assay. Briefly, BHK-21 cells (10^5/mL) were seeded in a 24-well plate (Thermo Fisher Scientific, Waltham, MA, USA) in medium without antibiotics at 37 °C with 5% CO_2 for 24 h. Then, the cells were incubated with GXYX crude lipopeptides (0.04, 0.08 or 0.2 mg) for 45 min and infected with *S*. Typhimurium for 1 h before subsequent assays. In the adhesion assay, after the medium was discarded, the cells were washed twice with PBS to eliminate unbound *S*. Typhimurium and then lysed with 0.1% Triton X-100 (Aladdin-reagent, Shanghai, China) for 15 min. Then, the diluted lysates were cultured on SS agar plates. After 24 h of cultivation, the number of viable colony-forming units (CFU) was determined. In the invasion assay, the medium was removed, and the cells were washed three times in PBS and then incubated for 1 h at 37 °C with DMEM containing 100 μg/mL gentamicin (Sigma–Aldrich, St. Louis, MI, USA) to remove extracellular bacteria. The medium was removed, and the cells were washed twice with PBS and then lysed with 0.1% Triton X-100 for 15 min. Finally, the collected lysis solution was serially diluted and plated onto *Salmonella Shigella* (SS) agar plates for bacterial counting after 24 h of incubation at 37 °C. Each assay was repeated three times. The control, which contained *S*. Typhimurium-infected BHK-21 cells, was used to define 100% adhesion or invasion. The results are presented as the percentage of relative inhibition of *S*. Typhimurium adhesion or invasion compared to that in the control group.

2.11. Animal experimental design

One hundred and twenty 6-week-old BALB/c specific pathogen-free (SPF) mice (60 male and 60 female) were purchased from Chengdu Dossy Experimental Animals Co., Ltd. (Sichuan, Chengdu, China) and randomly allocated to twelve groups (n = 10/group). Group A was preadministered 10 mg/kg GXYX crude lipopeptide via orogastric gavage (OG), and group B was preadministered 10 mg/kg GXYX crude lipopeptide via the intraperitoneal (IP) route. After three consecutive days of pretreatment with GXYX crude lipopeptides, groups A-C were challenged with 200 μL of 3.76×10^8 CFU/mL *S*. Typhimurium via the IP route. Group C served as a positive control. Group D served as a negative control and was treated with 200 μL phosphate-buffered saline (PBS) via the IP route. All the mice were euthanized on day 7 pi. The animal experimental design used to evaluate the effect of the GXYX crude lipopeptide on *S*. Typhimurium in groups A-D is shown in Fig. 7A. Groups E-G were subjected to in vivo toxicity assessment via the GXYX crude lipopeptide assay. Group E mice were pretreated with 10 mg/kg GXYX crude lipopeptide via orogastric gavage, group F mice were pretreated with 10 mg/kg GXYX crude lipopeptide via intraperitoneal injection, and group G mice were pretreated with 10 mg/kg PBS (pH: 7.2) via intraperitoneal injection. To determine the 50% lethal dose (LD_{50}) of *S*. Typhimurium, five groups of mice (H-L) were infected intraperitoneally (IP) with 200 μL of serial 10-fold dilutions of *S*. Typhimurium (ranging from 10^6 to 10^{10} CFU/mL). Mortality was monitored daily for 10 days after infection, and the LD_{50} was calculated by the Reed and Muench method [13]. All the mice were euthanized on day 10 pi. The detailed process related to the OG route was performed as follows: first, the mice were restrained so that their head and body were straight. Then, the stainless-steel feeding needle was inserted into the mouse mouth over the tongue. Once the needle was in place, the needle and syringe were inserted, and the needle was pressed gently against the palate so that the mouse's nose was toward the ceiling. The needle was redirected slightly as it passed through the back of the throat. The needle was continued until the stomach was reached. Then, the syringe was pushed to ensure that the GXYX crude lipopeptide flow into the stomach.

2.12. Clinical signs score

During the infection process, the following clinical signs were evaluated: listlessness, rough hair, loss of appetite, uncoordinated movements in the cage, diarrhea, mucus in the stool, weight loss, etc. The clinical signs and scores were evaluated and are described and scored in Table S1 in the Supplementary Material. The scores were summed, and the more signs there were, the higher the score was [4].

2.13. Hemolytic activity

The hemolytic activity of GXYX crude lipopeptides was evaluated by a hemoglobin release assay [14]. Fresh mouse erythrocytes were washed and centrifuged, after which red blood cells (RBCs) were obtained. The RBCs were rinsed and resuspended in PBS to obtain a 4% (v/v) suspension. The suspension was incubated with GXYX crude lipopeptides at various concentrations (0.0625–8 mg/mL), negative control solution (normal saline) or positive control solution (0.1% Triton X-100) for 1 h at 37 °C, after which the absorbance was measured at 570 nm. The percent hemolysis was calculated as follows: % hemolysis = [(OD_{570} with GXYX crude lipopeptides - OD_{570} normal saline)/(OD_{570} 0.1% Triton X100-OD_{570} normal saline)]. The average value was calculated from triplicate assays.

2.14. Transcript levels of cytokines and gut barrier-related genes determined by real-time fluorescence quantitative PCR (RT–qPCR)

The transcript levels of cytokines (IL-1β, IL-6, IL-12 and TNF-α) and gut barrier-related genes (ZO-1, claudin-1, and occludin-1) were tested using RT–qPCR. The fold changes in gene expression were normalized to that of β-actin and calculated using the

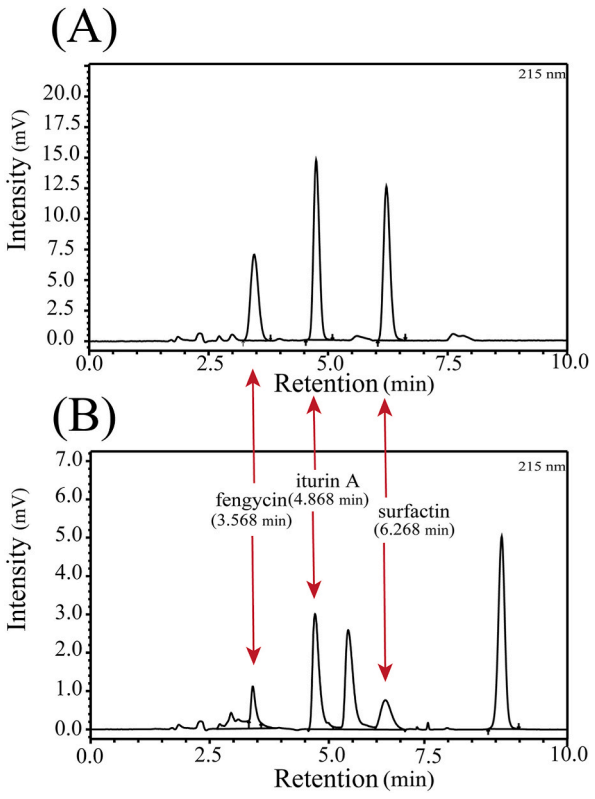

Fig. 1. The comparison of standard mixture of fengycin, iturin A, and surfactin, and GXYX crude lipopeptides with HPLC. The peaks of fengycin, iturin A, and surfactin are marked with arrows, and the retention time of fengycin, iturin A, and surfactin standards were 3.568, 4.868 and 6.268, respectively. (A) Chromatogram of a standard mixture of fengycin, iturin A, and surfactin, each at a concentration of 1 mmoL. (B) Chromatogram of GXYX crude lipopeptides.

$2^{-\Delta\Delta CT}$ method by the formula $\Delta\Delta Ct$ = mean ($\Delta Ct_{treated\ sample}$) -mean ($\Delta Ct_{untreated\ sample}$), $\Delta Ct = Ct_{target\ gene}$ - $Ct_{\beta\text{-actin}}$. The mean CT values ± standard deviations were calculated for the ΔΔCT data. The primers used are listed in Table 1.

2.15. Organ bacterial loads

The liver, spleen, kidney, and cecum were collected and homogenized at 0.1 mg/mL equivalent in sterile PBS (pH 7.2) and serially diluted 1:10 in sterile PBS, after which 100 μL was plated on SS plates. After 24 h at 37 °C in a static incubator (DPX-9052B; Nanrong Lab Equipment, Inc., Shanghai, China), the colonies were counted; the data are presented as the means ± SDs of triplicate samples and represent at least three independent experiments.

2.16. Histopathological examinations

Duodenal, liver, and spleen tissues from group E-G mice were removed, fixed in 4% paraformaldehyde for 24–48 h, processed routinely, sliced into 4 μm sections, and stained with hematoxylin and eosin (H&E). The histopathological lesions were examined via microscopy.

2.17. Statistical analysis

The results are expressed as the means with standard deviation (SD). Statistical analysis was carried out with one-way ANOVA and two-way ANOVA followed by multiple comparisons using GraphPad Prism v 7.04 (GraphPad software, San Diego, CA, USA). A P value < 0.05 was considered to indicate statistical significance. $^{****}P < 0.0001$, $^{***}P < 0.0001$. 001, $^{**}P < 0.01$, $^{*}P < 0.05$.

3. Results

3.1. RP-HPLC analysis

Three groups of crude lipopeptides produced by *B. subtilis* GXYX were initially detected with Rf values of 3.568, 4.868 and 6.268,

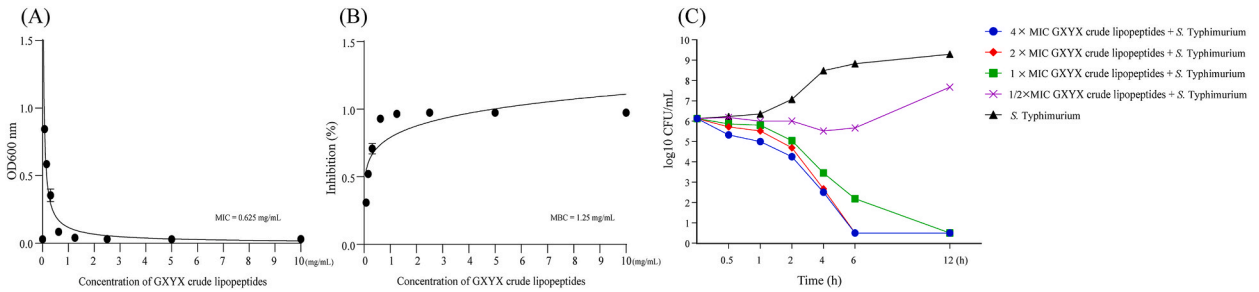

Fig. 2. (A) The MIC of GXYX crude lipopeptides. (B) The MBC of GXYX crude lipopeptides. (C) The antibacterial kinetic curves of GXYX crude lipopeptides against *S*. Typhimurium. The data are expressed as the mean ± SD (n = 3). *$P < 0.05$, ** $P < 0.01$, *** $P < 0.001$, **** $P < 0.0001$.

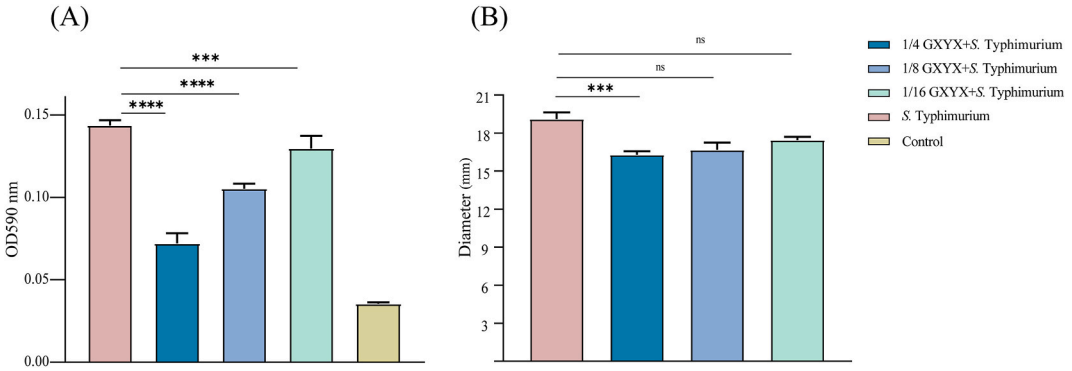

Fig. 3. (A) Effects of GXYX crude lipopeptides on *S*. Typhimurium biofilm formation. (B) Effects of GXYX crude lipopeptides on the motility of *S*. Typhimurium on agar plates. The data are expressed as the mean ± SD (n = 3). *$P < 0.05$, ** $P < 0.01$, *** $P < 0.001$, **** $P < 0.0001$.

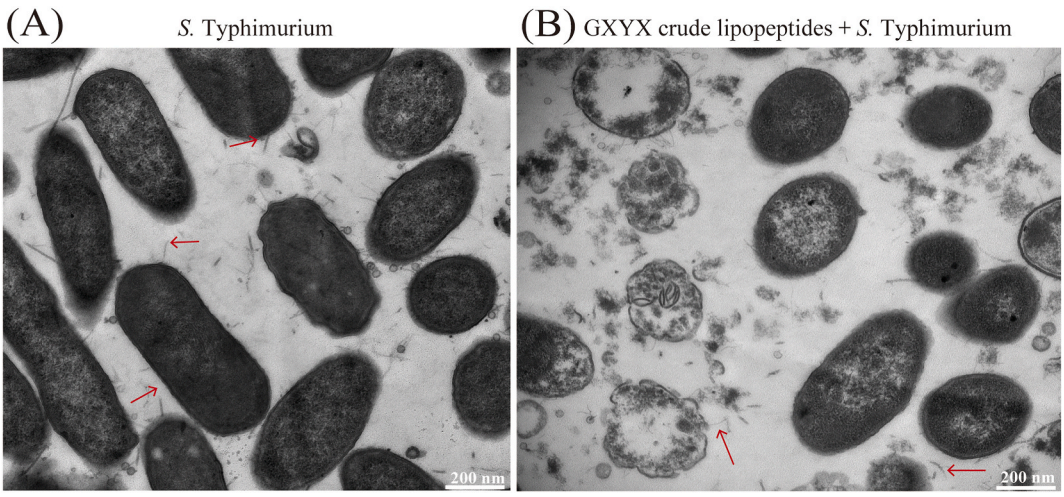

Fig. 4. TEM (30000 ×) analysis revealed that GXYX crude lipopeptide treatment relieved the intestinal ultrastructural changes caused by *S*. Typhimurium ATCC14028 in mice. (A) TEM image of *S*. Typhimurium. (B) TEM image of GXYX crude lipopeptide + *S*. Typhimurium.

which corresponded to fengycin, iturin A, and surfactin, respectively, according to the standards (Fig. 1A). The results indicated that *Bacillus subtilis* GXYX could produce lipopeptides, fengycin, iturin A and surfactin (Fig. 1B).

3.2. Characterization of GXYX crude lipopeptides against S

Typhimurium in vitro The MIC (Fig. 2A) and MBC (Fig. 2B) of GXYX crude lipopeptides against *S*. Typhimurium were 0.625 and 1.25 mg/mL, respectively. The time–kill curve (Fig. 2C) showed that GXYX crude lipopeptides induced rapid bactericidal effects at

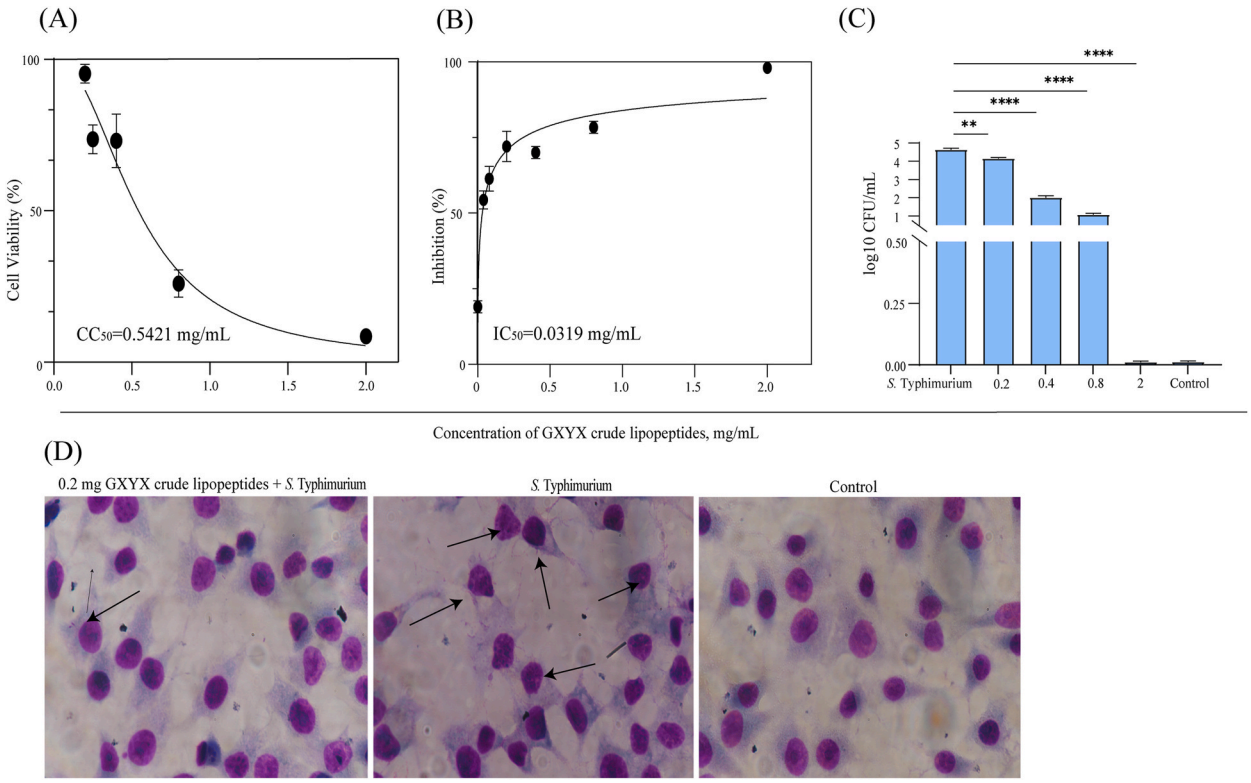

Fig. 5. (A) The cytotoxic concentration (CC_{50}) of GXYX crude lipopeptides against *S*. Typhimurium infection. (B) The half maximal inhibitory concentration (IC_{50}) of GXYX crude lipopeptides against *S*. Typhimurium infection. BHK-21 cells were co-incubated with *S*. Typhimurium at 10^6 CFU/mL and with the indicated concentrations of GXYX crude lipopeptide for 24 h. Subsequently, the cells were washed and incubated with 100 μL/well MTT reagent for 2 h. The CC_{50} and IC_{50} were determined from dose–response curves based on treatment with the indicated concentrations. (C) Dose-dependent inhibitory effect of GXYX crude lipopeptides on *S*. Typhimurium growth. (D) Wright–Giemsa staining (40 ×) of BHK-21 cells after 24 h of incubation with 0.2 mg of GXYX crude lipopeptide and *S*. Typhimurium; blue indicates cells, purple indicates bacteria. The solid black arrows indicate intracellular *S*. Typhimurium. The data are expressed as the mean ± SD (n = 3). * $P < 0.05$, ** $P < 0.01$, *** $P < 0.001$, **** $P < 0.0001$. (For interpretation of the references to color in this figure legend, the reader is referred to the Web version of this article.)

concentrations equal to or above the MIC for *S*. Typhimurium within 6 h in a dose-dependent manner. Compared to *S*. Typhimurium without GXYX crude lipopeptides, the growth of *S*. Typhimurium was inhibited at concentrations of GXYX greater than or equal to 1/2 MIC (Fig. 2C) ($P < 0.05$). *S*. Typhimurium biofilm formation was assessed in vitro using the classical crystal violet method. As shown in Fig. 3A, the GXYX crude lipopeptide significantly inhibited *S*. Typhimurium biofilm formation in a dose-dependent manner. The highest inhibition of *S*. Typhimurium was 38.5 ± 1.2% at 1/4 MIC. The motility of *S*. Typhimurium facilitates adherence to cells and destruction of the intestinal barrier. *S*. Typhimurium could cover a 19.21 mm plate surface within 12 h. At 1/16 MIC and 1/8 MIC, *S*. Typhimurium occupied the full plate surface at 17.44 mm and 16.5 mm, respectively (Fig. 3B). GXYX crude lipopeptides significantly inhibited *S*. Typhimurium motility in a dose-dependent manner. The TEM results showed that GXYX crude lipopeptides affected the number and structure of *S*. Typhimurium flagella. Numerous flagella surround each cell of *S*. Typhimurium (Fig. 4A). *S*. Typhimurium exhibited a normal rod shape with undamaged inner and outer membrane structures. The contents of the cells appeared to be well maintained, with the cytoplasmic membrane near the cell wall (Fig. 4A). With GXYX crude lipopeptide treatment, some flagella were disrupted. The cell envelope ruptures, causing the intracellular contents to drain. Many abnormal cells and many cells without membranes were observed (Fig. 4B). GXYX crude lipopeptides downregulated the transcription of flagella (*filA* and *filC*)- and biofilm (*csgA* and *csgB*)-related genes in a dose-dependent manner (Fig. S1).

3.3. GXYX crude lipopeptides inhibited S

Typhimurium growth in BHK-21 cells The CC_{50} of the GXYX crude lipopeptide was 0.5615 mg/mL (Fig. 5A), and the IC_{50} of the GXYX crude lipopeptide was 0.0319 mg/mL (Fig. 5B). The selectivity index (CC_{50}/IC_{50}) of the GXYX crude lipopeptide was 17.60. When the concentration of GXYX crude lipopeptide was 0.20 mg/mL, the cell survival rate was greater than 95%. After treatment with 0.2, 0.4, 0.8, or 2 mg/mL GXYX crude lipopeptide, the bacterial counts of *S*. Typhimurium decreased by 2.89%, 7.62% and 30.96%, respectively, compared with those in the control group, suggested GXYX crude lipopeptide inhibited *S*. Typhimurium growth in cell in a dose-dependent manner (Fig. 5C). Giemsa staining was used to observe morphological changes in BHK-21 cells (Fig. 5D). The

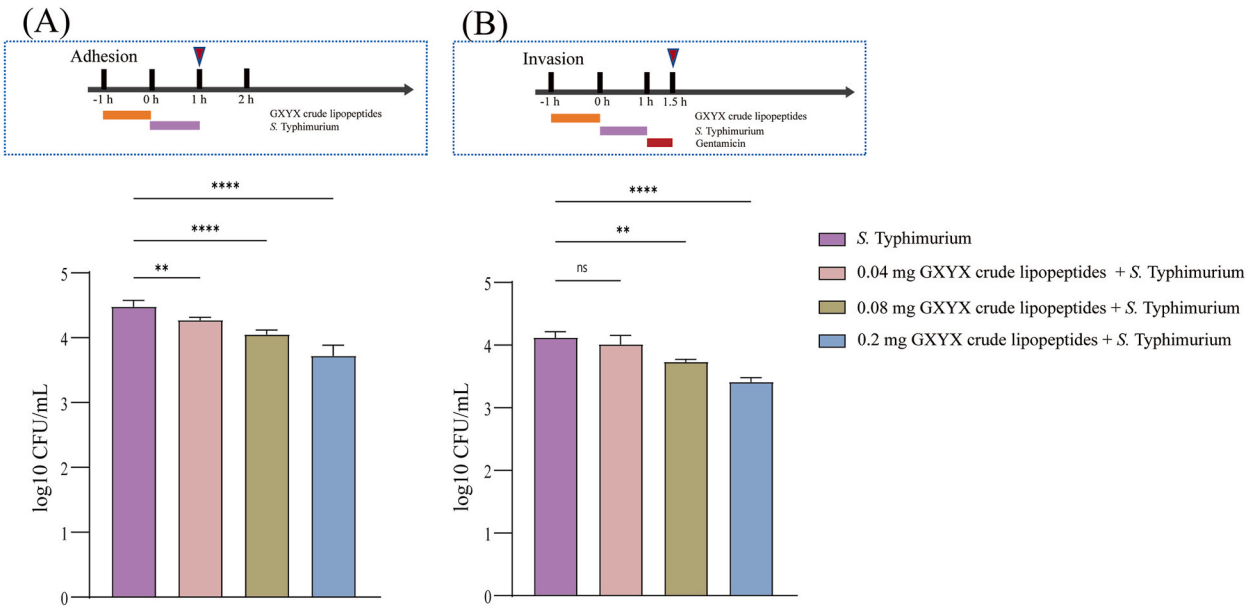

Fig. 6. Effects of GXYX crude lipopeptides on the ability of S. Typhimurium to adhere to and invade BHK-21 cells. (A) Adhesion; (B) invasion. The data are expressed as the mean ± SD (n = 3). * $P < 0.05$, ** $P < 0.01$, *** $P < 0.001$, **** $P < 0.0001$.

structure of the negative control cells was clear, and the chromatin staining was uniform, whereas the cells infected with *S*. Typhimurium showed chromatin condensation in the nuclei, a damaged structure, and increased staining. Compared to *S*. Typhimurium without GXYX crude lipopeptides, the addition of 0.2 mg of GXYX crude lipopeptides resulted in a small amount of *S*. Typhimurium invading the cells (Fig. 5D).

3.4. GXYX crude lipopeptides inhibited the adhesion and invasion of S

Typhimurium in a cell model As shown in Fig. 6, GXYX crude lipopeptide inhibited *S*. Typhimurium invasion (Fig. 6B) better than *S*. Typhimurium adhesion (Fig. 6A) to BHK-21 cells. With 0.2, 0.08, and 0.04 mg/mL GXYX crude lipopeptide treatment, the inhibition of *S*. Typhimurium adhesion was 16.92, 9.57 and 4.60%, respectively. In the invasion assay, GXYX crude lipopeptide inhibited 21.3, 6.9 and 5.0% of the *S*. Typhimurium strains at 0.2, 0.08, and 0.04 mg/mL, respectively.

3.5. GXYX crude lipopeptide treatment affected the survival rate and bacterial burden of mice infected with S

Typhimurium GXYX crude lipopeptides (0.25 mg/mL) caused less than 5% hemolysis (Fig. 7B). Here, 0.25 mg/mL GXYX crude lipopeptide was used as the experimental concentration. Mice were injected intraperitoneally with 0.25 mg of GXYX crude lipopeptide, and no signs, such as abnormal behavior, abnormal feeding or depression, were observed. H&E-stained histopathology revealed that the duodenum, liver and spleen of the mice in group A (OG) and group B (IP) had no abnormalities, suggesting that 0.25 mg of GXYX crude lipopeptide had no toxic effect on the mice (Fig. 7C). As shown in Fig. 8A, the LD_{50} of S. Typhimurium used in this study was 10^7 CFU/mL. Upon S. Typhimurium infection, the mice in group C displayed a range of clinical signs, including poor appetite, weakness, rough hair, diarrhea, and dyspnea. One day after infection, most of the mice in this group lost vigor and vitality and started losing weight, with the most severe signs appearing on the 4th day after infection (Fig. 8C); 50% of the mice survived (5 out of 10 died) throughout the entire experiment (Fig. 8B). All the mice that survived in the negative control group (D) showed no clinical signs (Fig. 8C). Clinical signs in the group B mice (intraperitoneal injection) included loss of appetite, lethargy, untidy coat, and diarrhea and were observed at 1 dpi. As time progressed, there was no significant improvement in these signs (Fig. 8C), and the mortality rate was also 30 % (Fig. 8B). Mice in group A were treated with GXYX crude lipopeptide via the OG route, and the symptoms were mild in the first 3 days. The sign score was significantly lower than that of group C (Fig. 8C). On the 5th day, the mice showed no signs of salmonellosis, and the mortality rate was 20 %. Orogastric gavage of GXYX crude lipopeptide improved the survival rate of the mice by 30% (Fig. 8B). Infection with *S*. Typhimurium induced bacterial translocation to the spleen and liver. Herein, we examined the effect of GXYX crude lipopeptides on *S*. Typhimurium colonization in the liver, spleen, kidney, and cecum. Compared with those in the *S*. Typhimurium infection group C, the bacterial burdens in the liver, spleen, kidney, and cecum in group A were significantly lower (40.60, 36.81, 44.12, and 33.42%, respectively). Compared to those in group C, the bacterial levels in the liver, spleen, kidney, and cecum in group B were 16.53, 11.12, 7.64, and 1.70%, respectively, lower. The bacterial loads in the liver, spleen, kidney, and cecum of group A were significantly lower than those in group B (Fig. 8D; $P < 0.05$).

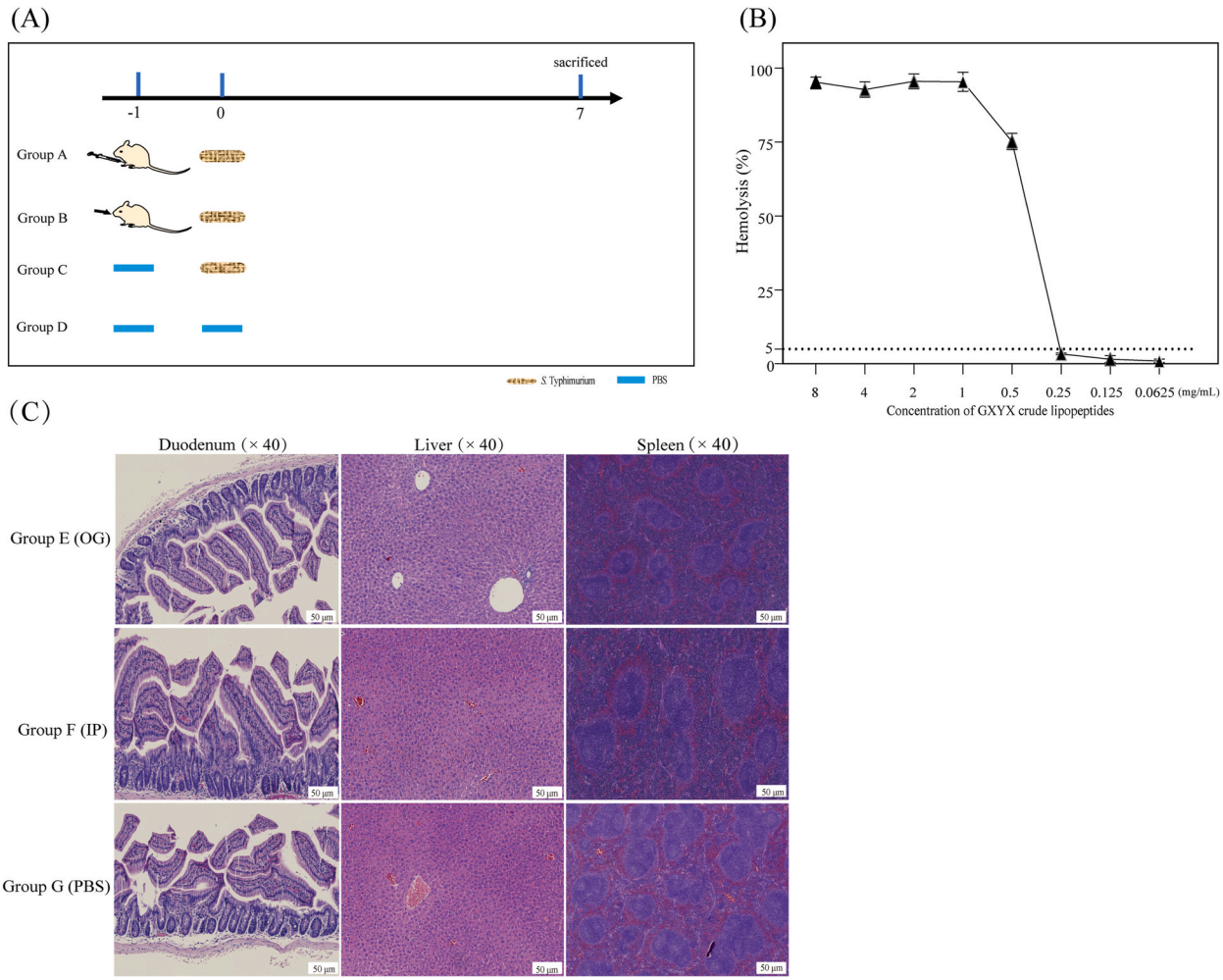

Fig. 7. (A) Animal experiment schematic for groups A-D. (B) The hemolytic activity of GXYX crude lipopeptides. Hemolytic activity was determined in mouse erythrocytes (4% suspended in PBS) after exposure to the GXYX crude lipopeptides at the indicated concentrations for 1 h. (C) Histological analysis of liver, spleen, and duodenum tissues from groups E, F and G mice to evaluate the safety of GXYX crude lipopeptides. (40 ×). The data are expressed as the mean ± SD (n = 3). * $P < 0.05$, ** $P < 0.01$, *** $P < 0.001$, **** $P < 0.0001$.

3.6. GXYX crude lipopeptide treatment affects the expression of inflammatory cytokines and gut barrier-related genes induced by S

Typhimurium. Compared with those in group D, the mRNA levels of TNF-α, IL-1β, IL-12, and IL-6 in group C were increased 4.57-, 9.67-, 25.82- and 13.25-fold, respectively (Fig. 9). Specifically, compared to those in group C, the expression of TNF-α, IL-1β, IL-12, and IL-6 in group B (IP route) was 4.18-, 7.86-, 17.68- and 9.41-fold lower, respectively, than that in group A, and the expression of TNF-α, IL-1β, IL-12, and IL-6 in group A (OG route) was downregulated 3.36-, 5.39-, 9.35- and 5.63-fold, respectively. In addition, S. Typhimurium infection decreased the mRNA levels of gut barrier-related genes (ZO-1, claudin-1, and occludin-1), and GXYX crude lipopeptide treatment inhibited these decreases, especially via the OG route (Fig. S2).

4. Discussion

Currently, there is increased concern about discovering a safe alternative approach for preventing pathogens. *Bacillus subtilis* and its metabolites are considered efficient ways to protect against pathogen invasion [15,16]. In this work, the potential of a novel *B. subtilis* strain, GXYX, to produce lipopeptides to control *S*. Typhimurium was investigated.

As previously reported, surfactin disrupted lipid structure through hydrophobic interactions and generated pores in bacterial membranes. Then, surfactin penetrates the bacterial membrane and changes the thickness of various bilayer membranes, leading to bacterial lysis [17,18]. Fengycins are cyclic lipopeptides that possess antifungal and antibacterial effects against pathogens [19,20]. In addition, iturin A, a highly effective lipopeptide that interacts with target membranes to form ionic pores in the membrane and increases the permeability of the pathogen membrane to potassium ions, exhibited significant antifungal effects and minimal toxicity

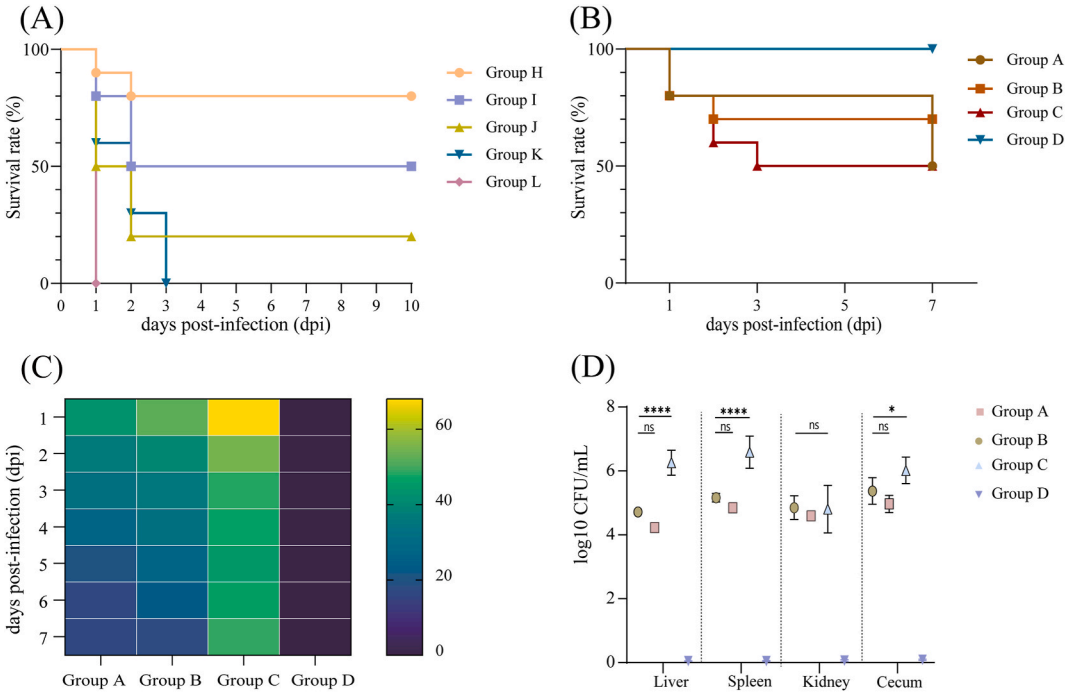

Fig. 8. GXYX crude lipopeptides relieved the damage caused by *S*. Typhimurium in mice. **(A)** The survival rate of mice treated with different doses (10^6–10^{10} CFU/mL) of *S*. Typhimurium was determined to determine the LD_{50} of *S*. Typhimurium in mice. (B) The survival rate of mice pretreated with GXYX before intraperitoneal administration of *S*. Typhimurium at the LD_{50}. (C) Heatmap of the clinical sign scores of mice from groups A-D. Yellow is associated with the highest score, and purple is the lowest score. The color scale ranges from purple to yellow for low to high average clinical scores. (D) The bacterial loads in the liver, kidney, spleen, and cecum of group A-D mice. The data are expressed as the mean ± SD (n = 3). * $P < 0.05$, ** $P < 0.01$, *** $P < 0.001$, **** $P < 0.0001$. (For interpretation of the references to color in this figure legend, the reader is referred to the Web version of this article.)

[21]. Here, GXYX produced fengycin, iturin A, and surfactin, which are lipopeptides that result in the inhibition of *S*. Typhimurium growth in vitro and in vivo, subsequently causing *S*. Typhimurium lysis and death [7,22].

The main antibacterial mechanism of *B. subtilis* crude lipopeptides is associated with disintegrating biological membranes and increasing the permeability of the bacterial membrane, which causes bacterial disruption and lysis of the membrane of pathogens [23,24]. A previous study revealed that lipopeptide-generated antibiofilm activity against *S*. Typhimurium and *Staphylococcus aureus* [25]. However, the potent antibacterial mechanisms of the GXYX crude lipopeptide against *S*. Typhimurium should be further investigated. *S*. Typhimurium relies on the motility of flagella to reach the target location [26]. The bacteria depend on the surface pilus to attach to cells [27,28]. They also form biofilms via extracellular matrices such as the pilus, which helps cells firmly colonize their surfaces. Furthermore, *S*. Typhimurium biofilm formation can enhance resistance to harsh conditions and antibacterial therapy [29]. The results showed that GXYX crude lipopeptides could inhibit *S*. Typhimurium swimming, cell adhesion and invasion, and biofilm formation. GXYX crude lipopeptides significantly inhibited the motility of *S*. Typhimurium flagella, thereby weakening their ability to swim in the medium. Furthermore, GXYX crude lipopeptides significantly inhibited the adhesion and invasion of *S*. Typhimurium to BHK-21 cells. The results showed that GXYX crude lipopeptides could significantly inhibit *S*. Typhimurium growth by reducing biofilm formation. Moreover, GXYX crude lipopeptides significantly inhibited the expression of multiple adhesion-related genes, such as flagella (*filA* and *filC*) and biofilms (*csgA* and *csgB*), which was consistent with the in vitro phenotypic results.

In the mammalian gut, the mucus layer on the gut epithelial surface could serve as the first physical barrier to limit the entry of bacterial toxins and pathogens [30]. The intestinal barrier, formed by epithelial cells and tight junction proteins (TJs), contributes to the protection and regulation of intestinal homeostasis [31]. TJs consist of multiple transmembrane proteins (such as claudins and occludin) and peripheral cytoplasmic scaffold proteins (zonula occludens and ZO-1) [31]. The destruction of TJs affects intestinal barrier integrity and permeability, causing inflammatory responses. Indeed, maintaining TJ protein expression could regulate barrier integrity and reduce pathogen-induced intestinal damage [31]. In addition, lipopeptides can strengthen the mucosal barrier of mice to defend against invading pathogens [32]. In our study, the mRNA levels of TJ proteins (ZO-1, claudins, occludin) were downregulated after *S*. Typhimurium infection, and GXYX crude lipopeptide pretreatment reversed this trend.

Epithelial barrier destruction can prime excessive inflammatory and immune responses by *S*. Typhimurium invading the intestinal mucosa [30]. The overexpression of inflammatory cytokines is the major biomarker of exacerbated intestinal inflammatory responses [33]. *S*. Typhimurium infection causes a strong inflammatory response and induces the production of inflammatory cytokines such as TNF-α, IL-1β, IL-12, and IL-6 [31,32]. TNF-α mainly mediates inflammation, immunity and apoptosis [34]. IL-1β is primarily

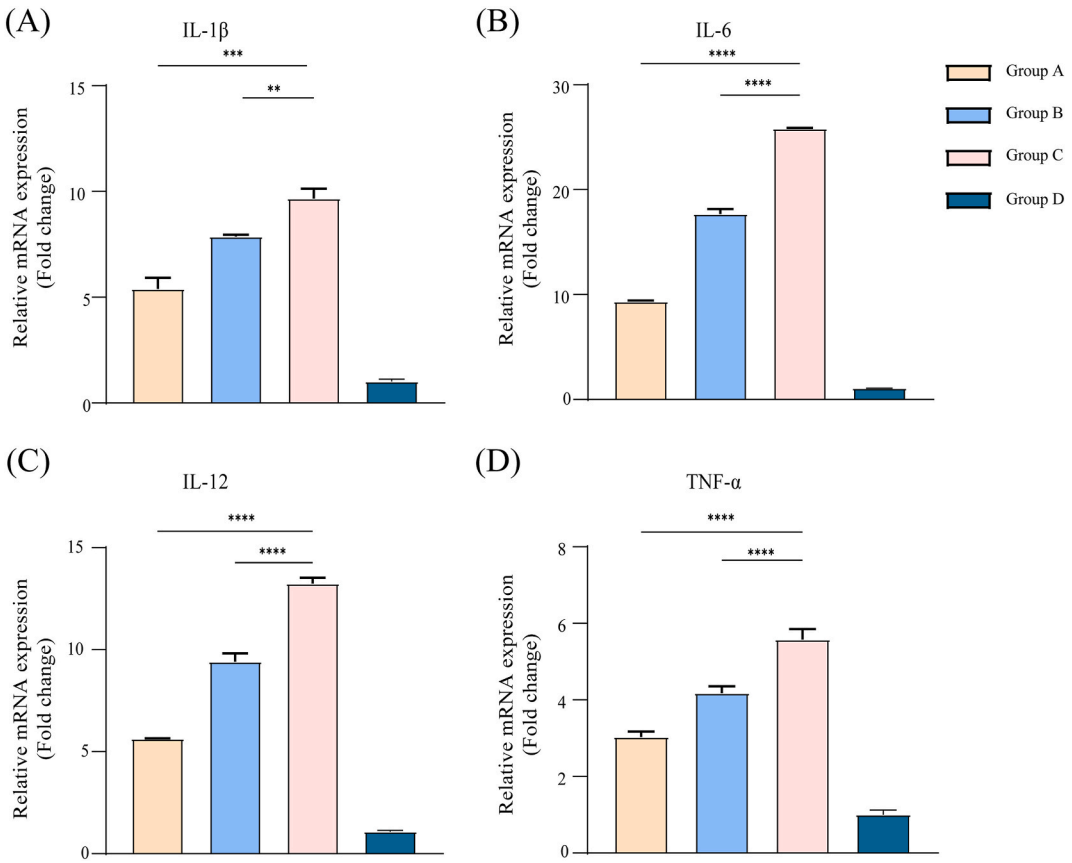

Fig. 9. GXYX crude lipopeptides reduced the mRNA expression of inflammatory factors (IL-1β (A), IL-6 (B), IL-12 (C) and TNF-α (D)) in *S.* Typhimurium-infected mice. All the experiments were repeated in triplicate. The data are expressed as the mean ± SD (n = 3). * $P < 0.05$, ** $P < 0.01$, *** $P < 0.001$, **** $P < 0.0001$.

responsible for triggering the inflammatory response characteristic of salmonellosis [35]. IL-12 is a key factor that drives Th1 responses and IFN-γ production and may activate MΦs and augment cell-mediated immunity while ultimately shaping antigen-specific immune responses [36]. IL-6 mediates the systemic effects of inflammatory processes [37]. In the present study, *S.* Typhimurium upregulated the mRNA levels of inflammatory factors (TNF-α, IL-1β, IL-12, and IL-6), which participate in activating the inflammatory response. Pretreatment with GXYX crude lipopeptide attenuated intestinal inflammation by downregulating the expression of inflammatory factors, and a better inhibitory effect was exhibited via OG than via the IP route. Therefore, these findings indicated that GXYX could significantly reduce the ability of *S.* Typhimurium to infect cells, inhibit the production of inflammatory cytokines, and ameliorate disrupted intestinal barrier damage.

Further evaluation of the safety of GXYX crude lipopeptides is essential for their future applications. The production of lipopeptides by various *B. subtilis* strains is safe for mice when lipopeptides are administered at a certain concentration [38]. The present study demonstrated that mice pretreated with 10 mg/kg GXYX crude lipopeptide via the OG route presented milder signs and lower bacterial loads in different tissues. Importantly, there were no significant systemic pathological changes. These results suggested that GXYX crude lipopeptide at doses lower than or equal to 10 mg/kg seems safe for practical application.

In conclusion, these studies demonstrated that GXYX crude lipopeptide could be an ideal potential agent against *S.* Typhimurium.

Ethics statement

The study was conducted according to the guidelines of the Declaration of Helsinki and approved by the Animal Ethics Committee of Northwest A&F University (approval number DY2022009). Six-week-old mice were bred in specific pathogen-free animal houses. All the experimental procedures were executed in accordance with the guidelines and regulations issued by the Standardization Administration of China.

Funding

This project was supported by the National Natural Science Foundation of China (Grant No. 31672581).

Informed consent statement

Not applicable.

Data availability statement

The data that support the findings of this study are available from the corresponding author upon reasonable request.

CRediT authorship contribution statement

Jingya Zhang: Writing – original draft, Validation, Software, Methodology, Investigation, Formal analysis, Data curation, Conceptualization. **Yifan Wu:** Software, Methodology, Investigation, Data curation. **Wei Li:** Visualization, Methodology, Investigation, Data curation. **Honglin Xie:** Validation, Software, Resources, Methodology, Conceptualization. **Jingyan Li:** Supervision, Software, Methodology, Investigation. **Yongqiang Miao:** Resources, Methodology. **Zengqi Yang:** Software, Methodology. **Yefei Zhou:** Software, Methodology. **Xinglong Wang:** Writing – review & editing, Writing – original draft, Supervision, Project administration, Investigation, Funding acquisition, Conceptualization.

Declaration of competing interest

The authors declare that they have no known competing financial interests or personal relationships that could have appeared to influence the work reported in this paper

Acknowledgments

Not applicable.

Appendix A. Supplementary data

Supplementary data to this article can be found online at https://doi.org/10.1016/j.heliyon.2024.e28219.

References

[1] P.R. Diaz, M.J. Torres, G. Petroselli, R. Erra-Balsells, M.C. Audisio, Antibacterial activity of Bacillus licheniformis B6 against viability and biofilm formation of foodborne pathogens of health importance, World J. Microbiol. Biotechnol. 38 (10) (2022) 181.
[2] J. Behnsen, A. Perez-Lopez, S.P. Nuccio, M. Raffatellu, Exploiting host immunity: the Salmonella paradigm, Trends Immunol. 36 (2) (2015) 112–120.
[3] W. Yang, Y. Cong, Gut microbiota-derived metabolites in the regulation of host immune responses and immune-related inflammatory diseases, Cell. Mol. Immunol. 18 (4) (2021) 866–877.
[4] B. Deng, J. Wu, X. Li, C. Zhang, X. Men, Z. Xu, Effects of Bacillus subtilis on growth performance, serum parameters, digestive enzyme, intestinal morphology, and colonic microbiota in piglets, Amb. Express 10 (1) (2020) 212.
[5] D. Konkol, I. Szmigiel, M. Domzal-Kedzia, M. Kulazynski, A. Krasowska, S. Opalinski, M. Korczynski, M. Lukaszewicz, Biotransformation of rapeseed meal leading to production of polymers, biosurfactants, and fodder, Bioorg. Chem. 93 (2019) 102865.
[6] A. El Arbi, A. Rochex, G. Chataigne, M. Bechet, D. Lecouturier, S. Arnauld, N. Gharsallah, P. Jacques, The Tunisian oasis ecosystem is a source of antagonistic Bacillus spp. producing diverse antifungal lipopeptides, Res. Microbiol. 167 (1) (2016) 46–57.
[7] J.P. Motta, J.L. Wallace, A.G. Buret, C. Deraison, N. Vergnolle, Gastrointestinal biofilms in health and disease, Nat. Rev. Gastroenterol. Hepatol. 18 (5) (2021) 314–334.
[8] X. Pierrat, J.P.H. Wong, Z. Al-Mayyah, A. Persat, The mammalian membrane microenvironment regulates the sequential attachment of bacteria to host cells, mBio 12 (4) (2021) e0139221.
[9] J.A. Horstmann, M. Lunelli, H. Cazzola, J. Heidemann, C. Kuhne, P. Steffen, S. Szefs, C. Rossi, R.K. Lokareddy, C. Wang, et al., Methylation of Salmonella Typhimurium flagella promotes bacterial adhesion and host cell invasion, Nat. Commun. 11 (1) (2020) 2013.
[10] S.D. Todorov, B.D.G. de Melo Franco, J.R. Tagg, Bacteriocins of Gram-positive bacteria having activity spectra extending beyond closely-related species, Benef. Microbes 10 (3) (2019) 315–328.
[11] H. Gong, X. Hu, M. Liao, K. Fa, D. Ciumac, L.A. Clifton, M.A. Sani, S.M. King, A. Maestro, F. Separovic, et al., Structural disruptions of the outer membranes of gram-negative bacteria by rationally designed amphiphilic antimicrobial peptides, ACS Appl. Mater. Interfaces 13 (14) (2021) 16062–16074.
[12] S. Arnaouteli, N.C. Bamford, N.R. Stanley-Wall, A.T. Kovacs, Bacillus subtilis biofilm formation and social interactions, Nat. Rev. Microbiol. 19 (9) (2021) 600–614.
[13] S.A. Saganuwan, Application of median lethal concentration (LC(50)) of pathogenic microorganisms and their antigens in vaccine development, BMC Res. Notes 13 (1) (2020) 289.
[14] M. Akbarian, S.H. Chen, M. Kianpour, F. Farjadian, L. Tayebi, V.N. Uversky, A review on biofilms and the currently available antibiofilm approaches: matrix-destabilizing hydrolases and anti-bacterial peptides as promising candidates for the food industries, Int. J. Biol. Macromol. 219 (2022) 1163–1179.
[15] F. Kaspar, P. Neubauer, M. Gimpel, Bioactive secondary metabolites from Bacillus subtilis: a comprehensive review, J. Nat. Prod. 82 (7) (2019) 2038–2053.
[16] R. Zhang, Z. Li, X. Gu, J. Zhao, T. Guo, J. Kong, Probiotic Bacillus subtilis LF11 protects intestinal epithelium against Salmonella infection, Front. Cell. Infect. Microbiol. 12 (2022) 837886.
[17] M.M. Mabrouk, S.M. Soliman, H.M. El-Agizy, F.R. Mansour, Ultrasound-assisted dispersive liquid-liquid microextraction for determination of three gliflozins in human plasma by HPLC/DAD, J. Chromatogr., B: Anal. Technol. Biomed. Life Sci. 1136 (2020) 121932.
[18] X. Wang, L. Liang, H. Shao, X. Ye, X. Yang, X. Chen, Y. Shi, L. Zhang, L. Xu, J. Wang, Isolation of the novel strain Bacillus amyloliquefaciens F9 and identification of lipopeptide extract components responsible for activity against xanthomonas citri subsp, citri. Plants 11 (3) (2022) (Basel).

[19] Q.Y. Zhang, Z.B. Yan, Y.M. Meng, X.Y. Hong, G. Shao, J.J. Ma, X.R. Cheng, J. Liu, J. Kang, C.Y. Fu, Antimicrobial peptides: mechanism of action, activity and clinical potential, Mil Med Res 8 (1) (2021) 48.
[20] M. Adnan, A.J. Siddiqui, W.S. Hamadou, S.A. Ashraf, M.I. Hassan, M. Snoussi, R. Badraoui, A. Jamal, F. Bardakci, A.M. Awadelkareem, et al., Functional and structural characterization of pediococcus pentosaceus-derived biosurfactant and its biomedical potential against bacterial adhesion, quorum sensing, and biofilm formation, Antibiotics (Basel) 10 (11) (2021).
[21] T. Li, L. Li, F. Du, L. Sun, J. Shi, M. Long, Z. Chen, Activity and mechanism of action of antifungal peptides from microorganisms: a review, Molecules 26 (11) (2021).
[22] Y. Fan, J. Qiao, Z. Lu, Z. Fen, Y. Tao, F. Lv, H. Zhao, C. Zhang, X. Bie, Influence of different factors on biofilm formation of Listeria monocytogenes and the regulation of cheY gene, Food Res. Int. 137 (2020) 109405.
[23] X. Zhao, X. Wang, R. Shukla, R. Kumar, M. Weingarth, E. Breukink, O.P. Kuipers, Brevibacillin 2V, a novel antimicrobial lipopeptide with an exceptionally low hemolytic activity, Front. Microbiol. 12 (2021) 693725.
[24] P. Laorodphun, R. Cherngwelling, A. Panya, P. Arjinajarn, Curcumin protects rats against gentamicin-induced nephrotoxicity by amelioration of oxidative stress, endoplasmic reticulum stress and apoptosis, Pharm. Biol. 60 (1) (2022) 491–500.
[25] H. Kimelman, M. Shemesh, Probiotic bifunctionality of Bacillus subtilis-rescuing lactic acid bacteria from desiccation and antagonizing pathogenic Staphylococcus aureus, Microorganisms 7 (10) (2019).
[26] C. Das, C. Mokashi, S.S. Mande, Saini S: **dynamics and control of flagella assembly in Salmonella typhimurium**, Front. Cell. Infect. Microbiol. 8 (2018) 36.
[27] P. Chakraborty, A. Kumar, The extracellular matrix of mycobacterial biofilms: could we shorten the treatment of mycobacterial infections? Microb Cell 6 (2) (2019) 105–122.
[28] L. Karygianni, Z. Ren, H. Koo, T. Thurnheer, Biofilm matrixome: extracellular components in structured microbial communities, Trends Microbiol. 28 (8) (2020) 668–681.
[29] K. Chen, Z. Zhan, L. Li, J. Li, Z. Zhou, N. Wang, D. Sun, C. Xu, P. Chen, X. Qu, et al., BolA affects the biofilm formation ability, outer membrane permeability and virulence, thus is required for the adaptability of Salmonella enterica serotype Typhimurium to the harsh survival environment, Microbiol. Res. 274 (2023) 127423.
[30] A. Ali, H. Tan, G.E. Kaiko, Role of the intestinal epithelium and its interaction with the microbiota in food allergy, Front. Immunol. 11 (2020) 604054.
[31] T. Suzuki, Regulation of the intestinal barrier by nutrients: the role of tight junctions, Anim. Sci. J. 91 (1) (2020) e13357.
[32] R.S. Patel, B. Agrawal, Mucosal immunization with lipopeptides derived from conserved regions of SARS-CoV-2 antigens induce robust cellular and cross-variant humoral immune responses in mice, Front. Immunol. 14 (2023) 1178523.
[33] C. Liu, D. Chu, K. Kalantar-Zadeh, J. George, H.A. Young, G. Liu, Cytokines: from clinical significance to quantification, Adv. Sci. 8 (15) (2021) e2004433.
[34] P. Zhou, S. Lu, Y. Luo, S. Wang, K. Yang, Y. Zhai, G. Sun, X. Sun, Attenuation of TNF-alpha-Induced inflammatory injury in endothelial cells by ginsenoside Rb1 via inhibiting NF-kappaB, JNK and p38 signaling pathways, Front. Pharmacol. 8 (2017) 464.
[35] T. Liu, L. Zhang, D. Joo, S.C. Sun, NF-kappaB signaling in inflammation, Signal Transduct. Targeted Ther. 2 (2017) 17023.
[36] S. Mukherjee, S. Karmakar, S.P. Babu, TLR2 and TLR4 mediated host immune responses in major infectious diseases: a review, Braz. J. Infect. Dis. 20 (2) (2016) 193–204.
[37] J. Schneiders, F. Fuchs, J. Damm, C. Herden, R. Gerstberger, D.M. Soares, J. Roth, C. Rummel, The transcription factor nuclear factor interleukin 6 mediates pro- and anti-inflammatory responses during LPS-induced systemic inflammation in mice, Brain Behav. Immun. 48 (2015) 147–164.
[38] S.S. Giri, E.C. Ryu, V. Sukumaran, S.C. Park, Antioxidant, antibacterial, and anti-adhesive activities of biosurfactants isolated from Bacillus strains, Microb. Pathog. 132 (2019) 66–72.